Coherence of subthreshold activity in coupled inferior olivary neurons

Anna Devor and Yosef Yarom. Dept. of Neurobiology, Hebrew Univ., Jerusalem, Israel

Introduction

Subthreshold membrane potential oscillations (STO) in the inferior olivary (IO) nucleus are believed to underlie synchrony and rhythmicity of complex spikes in the cerebellar cortex. Synchronous and rhythmic behavior of complex spikes is modulated either pharmacologically, by applying drugs directly to the IO nucleus (Lang 2001; Lang et al. 1996), or during motor behavior (Smith 1998; Welsh et al. 1995). In the present study we examined the stability of STO using slice preparations of the IO nucleus.

Lang E (2001) Organization of olivocerebellar activity in the absence of excitatory glutamatergic input. J Neurosci; 21: 1663-1675.

Lang EJ, Sugihara I, and Llinas R. (1996) GABAergic modulation of complex spike activity by the cerebellar nucleoolivary pathway in rat. *J Neurophysiol* 76: 255-275.

Smith SS (1998) Step cycle-related oscillatory properties of inferior olivary neurons recorded in ensembles. Neuroscience 82: 69-80.

Welsh JP, Lang EJ, Sugihara I, Llinas R (1995) Dynamic organization of motor control within the olivocerebellar system. Nature 374: 453-456.

Methods

Single and double patch recordings were performed in sagittal brain stem slices of 9-31 day old rats. The pipettes were filled with the intracellular solution (containing in mM: 4 NaCl, 10^{-3} $CaCl_2$, 140 K-gluconate, 10^{-2} EGTA, 4 Mg-ATP, 10 Hepes; pH 7.2). Time-frequency (TF) plots (Palva et al. 2000) are color coded representations of changes in frequency of STO in time. The amplitude scale of TF plots is in arbitrary units comparable between plots. The amplitude of crosscorrelograms is expressed in units of the correlation coefficient (rho).

Optical imaging was performed in brain slices using voltage sensitive styryl dye RH-414.

Palva JM, Lamsa K, Lauri SE, Rauvala H, Kaila K, Taira T (2000) Fast network oscillations in the newborn rat hippocampus *in vitro*. J Neurosci 30: 1170-1178.

Prevalence of STO

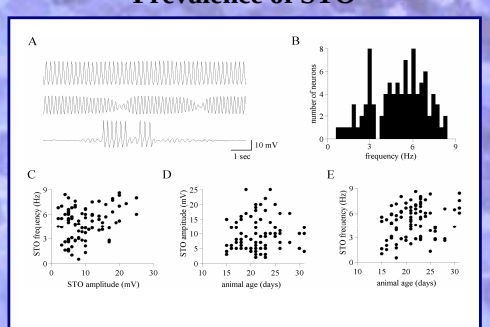

The frequency and amplitude distribution of STO in olivary neurons.

A. The spontaneous STO in olivary neurons appear at different frequency, pattern and amplitude. Traces were recorded from different neurons in different slices.

B. Distribution of average STO frequency in 94 neurons. Note two populations of frequencies separated at about 3.5 Hz.

C-E. Average frequency of STO, plotted as a function of STO maximal amplitude (C) or as a function of age of the animal (E), shows significant positive correlation, while STO maximal amplitude and the age of the animal are not correlated (D).

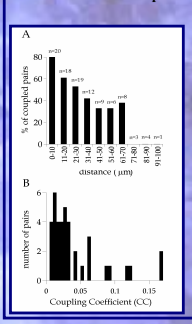

A. Possibility of finding a coupled cell pair as a function of distance between the cells.

B. Distribution of coupling coefficient (CC) in 20 pairs of electrotonically coupled neurons. The CC, defined as the ratio between voltage responses of the post- and the pre-juctional cell, varied between 0.002 and 0.17; most of the pairs were weakly coupled. In more than 75% of the pairs the CC was less than 0.05. Both CC upon current injection into cell 1 (CC_1) and into cell 2 (CC_2) are plotted in the same graph.

Variation of STO in the temporal domain

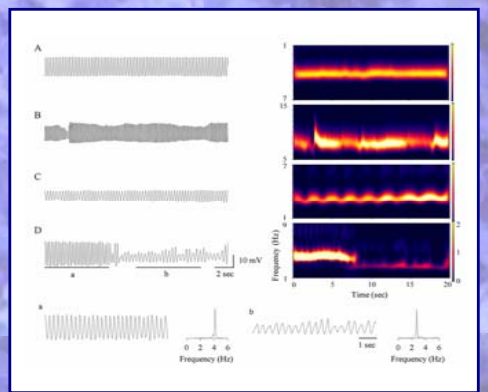

A.-C. The traces on the left were recorded from 3 different neurons in 3 different slices corresponding. TF analysis, shown on the right, demonstrates constant frequency in A and changing frequency in B and C. Changes in frequency were associated with changes in the amplitude (compare the trace on the left and its TF representation on the right). The amplitude is coded in color so that bright yellow corresponds to higher amplitude (see the color scale on he right).

D. Two-state oscillatory behavior in an IO neuron. The trace on the left and its TF representation on the right show a sudden shift from a higher to a lower frequency. The underlined time segments "a" and "b" are shown on a faster time scale at the bottom of the figure. Fourier analysis of each one of the segments (on the right) demonstrates the shift from about 4 to about 2.5 Hz.

Blocking spiking activity stabilizes the temporal pattern of STO

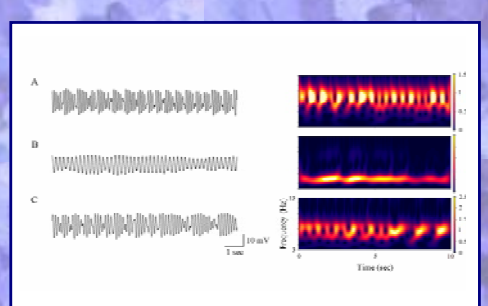

TTX stabilizes frequency and amplitude modulations of STO.

A. STO recorded under control conditions exhibited significant frequency and amplitude modulations.

B. Bath application of 0.5 μM of TTX largely abolished spontaneous shifts.

C. Washout of the drug restored the control behavior of STO. TF representations of the traces on the right show a complex pattern of frequency modulation before TTX application and after the washout, and a regular frequency of about 5 Hz following TTX.

CNQX stabilizes the temporal pattern of STO

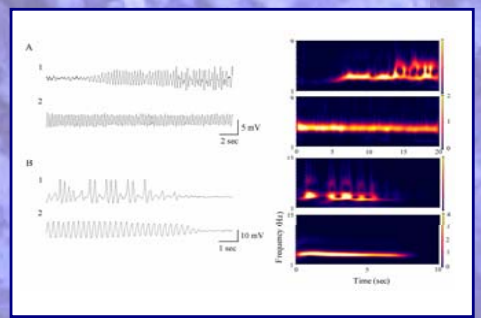

A. STO recorded before (trace 1) and 20 min after (trace 2) bath application of 40 μM of CNQX. TF representations of the traces on the right show a complex pattern of frequency modulation before CNQX application and a regular frequency of about 4 Hz following CNQX.

B. Second example of the effect of CNQX, in a neuron recorded from a different slice.

Coherence of STO in pairs of olivary neurons

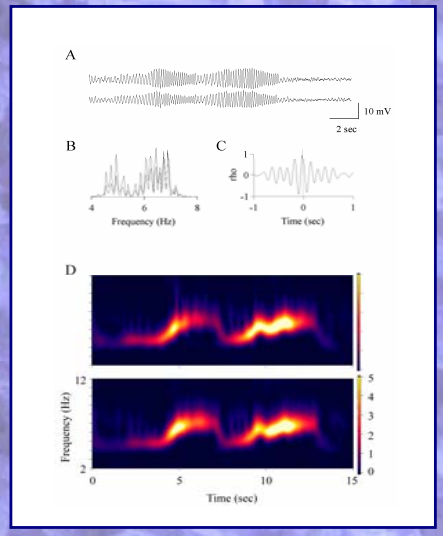

Complex pattern of STO modulation in non-coherent pairs.

A. Simultaneous recordings from two intermittently oscillating neurons. Note synchronous modulation in amplitude.

B. Fourier analysis shows almost identical spectra.

C. The crosscorrelation peak is shifted to the left indicating about 20 msec phase difference.

D. TF representation of the traces shown in A. Note synchronous modulations in frequency in both cells.

Optical imaging of propagating oscillations

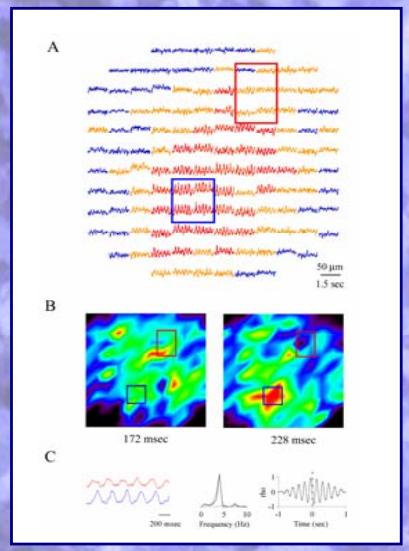

Optical imaging of spontaneous coherent oscillations.

A. Each trace represents the change in fluorescence recorded by a single photodiode in its relative location as a function of time. Fourier analysis was performed on all diodes. All diodes where the amplitude of the main frequency component was >= 30% of that of the best diode are marked in red. All diodes where the amplitude of the main frequency component was between 10% and 30% of that of the best diode are marked in yellow. Note the central patch of high amplitude oscillations.

B. Color coded activity over the whole array, measured at times denoted under the panels.

C. Red and blue traces on C represent averaged signals from diodes inside the red and blue frames, marked in both A and B. Fourier spectra and crosscorrelation of these averaged signals are shown in the middle and on the right, respectively.

Conclusions

Olivary oscillations exhibited unstable temporal patterns. This instability was significantly reduced following a block of synaptic transmission, implying that frequency and amplitude modulations are imposed on the olivary network by extrinsic synaptic inputs.

The size of the synchronously oscillating olivary population, as observed by optical imaging, was comparable to the size of the population that would create a parasagittal band of synchronously firing Purkinje cells.

Both pair recordings and optical imaging demonstrated phase shifted oscillatory activity along the olivary slice. These findings rise further questions about directional organization of information flow within the IO nucleus.

Acknowledgements

We are grateful to Matias Palva for providing TF analysis software, and to Hanoch Meiri for excellent technical assistance. This study was supported by the US-Israel Binational Science Foundation and the European Commission.